SUPPORTING INFORMATION

Understanding the Lithiation of Sn Anode for High Performance Li-ion Batteries with Exploration of Novel Li-Sn Compounds at Ambient and Moderately High Pressure

Raja Sen and Priya Johari*

Department of Physics, School of Natural Sciences,

Shiv Nadar University, Greater Noida,

Gautam Budhha Nagar, UP 201 314, India.

*Electronic address: priya.johari@snu.edu.in, psony11@gmail.com

Contents

1. Computational details

USPEX has already been demonstrated as a powerful tool to determine the lowest energy structure *via* global minimization of the surface free-energy, with great success.[1, 2] Our calculations to search for stable and metastable structures of Li-Sn compounds were carried out using USPEX in two steps. Firstly, most promising compositions of Li-Sn compounds were explored through variable composition method at 1 atm, 5, 10, and 20 GPa pressure considering up to 40 atoms per unit cell. The calculations were carried out over the course of 50-60 generations where, the first generation was generated randomly with 150-200 structures by sampling 20-25 different compositions. For the subsequent generations, 40 child structures were produced, through different symmetry generators, namely heredity, transmutation, softmutation, and random, with probabilities of 40%, 20%, 20%, and 20%, respectively. In second step, a fixed composition search of each promising stoichiometry of Li-Sn compounds with different number of formula units (depending upon the stoichiometry, it varies from 1 to 5) was carried out for over 30-40 generations, with 30-35 different structures in each generation. The population of first generation in fixed composition search was also set with 80-120 structures, in order to densely map the configuration space of random search.

In general, study of Gibbs free energy ($G = H - TS$; here H, T, and S describe the enthalpy, temperature and entropy, respectively, of the system) is the essential criterion to decide the thermodynamical stability of any compounds. However, DFT study always deals with 0 K temperature, implying $G = H$. Therefore, through out the manuscript we only discussed the enthalpies of the Li-Sn compounds at different pressure. Here, it is also believed that magnitude of vibrational energies (TS) towards total free energy would be negligibly small near room temperature and therefore can not change the order of thermodynamics of stability of Li-Sn compounds.

Therefore, negative enthalpy of formation which is the basic criterion for finding the energetically stable compounds was calculated *via* below equation:

$$\triangle H_f(Li_xSn_y) = \frac{[H(Li_xSn_y) - xH(Li) - yH(Sn)]}{(x+y)} \quad (1)$$

where, $H = U + PV$ is the enthalpy of each compositions in their crystal form and $\triangle H_f$ is the formation enthalpy of the compound per atom. In the expression of enthalpy, U, P, and V represent the internal energy, pressure, and volume, respectively.

It should be noted that for a given stoichiometry and pressure, the structure having lowest negative value of formation enthalpy can be considered as most favorable phase as compared to others. But, in order to judge the thermodynamic stability of a particular Li-Sn compound with respect to two nearest neighbor compositions and/or pure elements at ambient or high pressure, it is important to draw the thermodynamic convex hull. The thermodynamic convex hull which, is a representater of compound's formation enthalpy with its respective stoichiometric ratio at given pressure, is also able to elucidate the all possible decomposition routes. Basically, a phase can be identified as thermodynamically stable ground state phase if it lies on the convex hull. Hence, the stoichiometries that do not have a representative structure on the convex hull, are considered as either metastable or unstable. However, in order to govern the local (meta)stability, we further investigated the phonon dispersion curves of all respective Li-Sn compounds. A structure can be considered as dynamically stable, if and only if, no imaginary phonon frequencies are detected through out the Brillouin zone in phonon dispersion curve.

The structure relaxation of all compositions generated by USPEX were accomplished using first-principles density functional theory (DFT) with the atomic force convergence criterion of 0.001 eV/Å as implemented in the Vienna Ab-initio Simulation Package (VASP).[3, 4] The electron-ion interactions were treated using projector-augmented-wave (PAW) pseudo-potentials,[5] while, to account exchange correlation effects, the generalized gradient approximation (GGA) functional in PBE (Perdew–Burke–Ernzerhof) flavor was used.[6] The plane-wave kinetic energy cutoff was considered as 700 eV, while the reciprocal space resolution for k-points generation in final structures relaxation and enthalpy calculations was set to $0.02\times2\Pi$ $Å^{-1}$ with uniform $\Gamma-$ centered meshes. All the above mentioned parameters ensure that the enthalpy calculations are well converged with fluctuation in enthalpy to be less than 1 meV/atom. In order to probe the dynamical stability, phonon frequencies throughout the whole Brillouin Zone were calculated using density functional perturbation theory (DFPT) as implemented in the VASP code along with the Phonopy package.[7] Depending upon the primitive cells structure, $l \times m \times n$ supercells (where, $2 \leq l, m, n \leq 3$) were used to calculate the phonon dispersion curve. In addition, the theoretical gravimetric capacity, GC, was also determined using following equation:

$$\mathrm{GC} = \frac{\mathrm{xF}}{\mathrm{M_{Sn}}} \tag{2}$$

where, x is the number of Li atoms present in Li_xSn, F is the Faraday constant, and M_{Sn} represents the Molar-Mass of Sn.

To examine mechanical properties, elastic constants were calculated using the VASP code, while the bulk modulus (B), shear modulus (G), Young modulus (Y), and Poisson's ratio (ν) were estimated using the Voigt-Reuss-Hill approximation (Section 12 of SI).[8] Finally, in order to guide the synthesis of unknown Li-Sn compounds, X-ray diffraction powder patterns of all studied phases of Li-Sn were simulated via Mercury software (Figure S14 of SI).[9]

2. Phonon dispersion curves of Li-Sn compounds

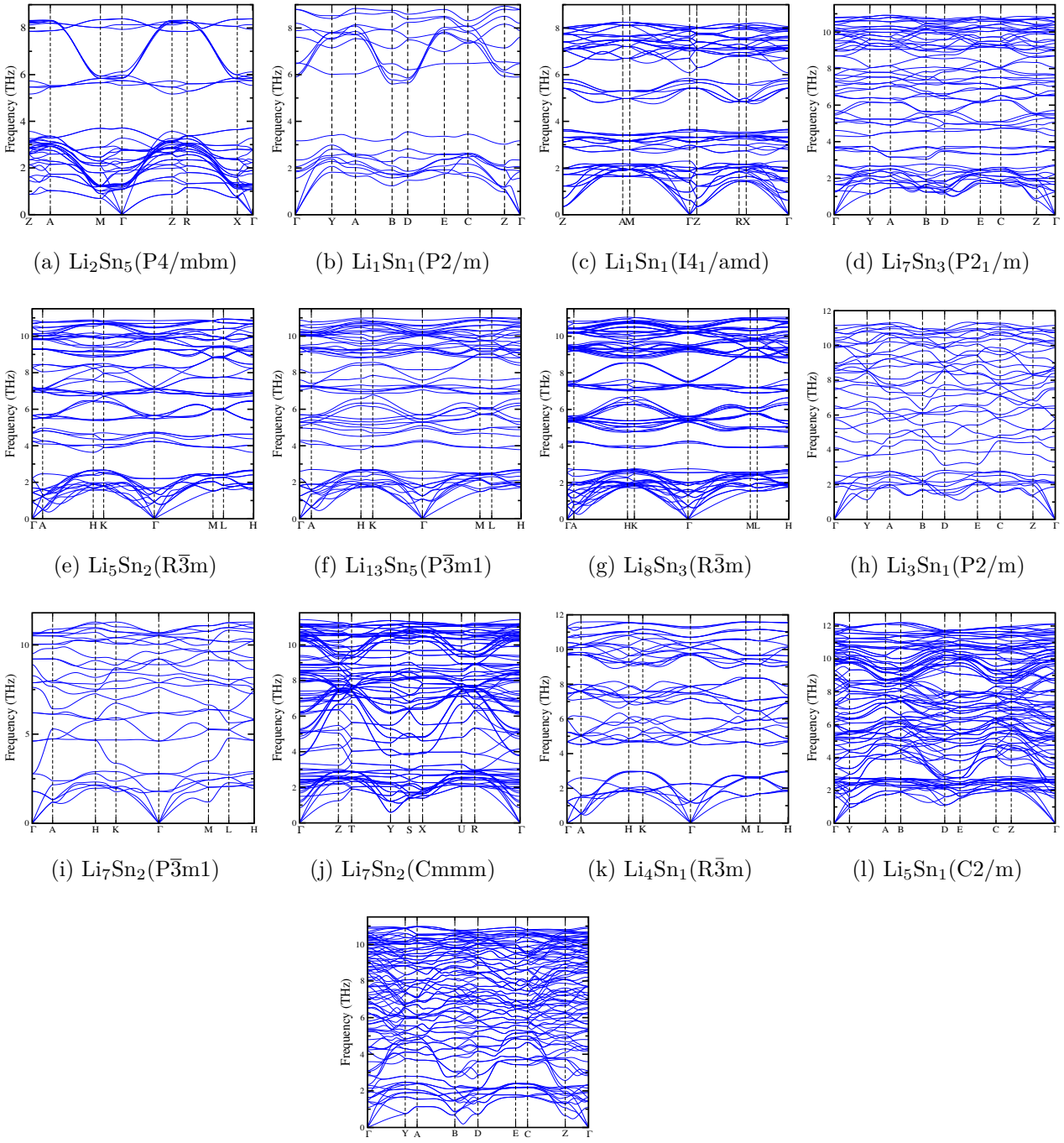

(a) Li_2Sn_5(P4/mbm) (b) Li_1Sn_1(P2/m) (c) Li_1Sn_1($I4_1$/amd) (d) Li_7Sn_3($P2_1$/m)

(e) Li_5Sn_2(R$\bar{3}$m) (f) $Li_{13}Sn_5$(P$\bar{3}$m1) (g) Li_8Sn_3(R$\bar{3}$m) (h) Li_3Sn_1(P2/m)

(i) Li_7Sn_2(P$\bar{3}$m1) (j) Li_7Sn_2(Cmmm) (k) Li_4Sn_1(R$\bar{3}$m) (l) Li_5Sn_1(C2/m)

(m) Li_7Sn_1(C2/m)

Figure S1: Phonon dispersion curves of: (a) Li_2Sn_5(P4/mbm), (b) Li_1Sn_1(P2/m), (c) Li_1Sn_1($I4_1$/amd), (d) Li_7Sn_3($P2_1$/m), (e) Li_5Sn_2(R$\bar{3}$m), (f) $Li_{13}Sn_5$(P$\bar{3}$m1), (g) Li_8Sn_3(R$\bar{3}$m), (h) Li_3Sn_1(P2/m), (i) Li_7Sn_2(P$\bar{3}$m1), (j) Li_7Sn_2(Cmmm), (k) Li_4Sn_1(R$\bar{3}$m), (l) Li_5Sn_1(C2/m) and (m) Li_7Sn_1(C2/m), appeared at 1 atm convex-hull. Curves are arranged in an increasing order of Li-content.

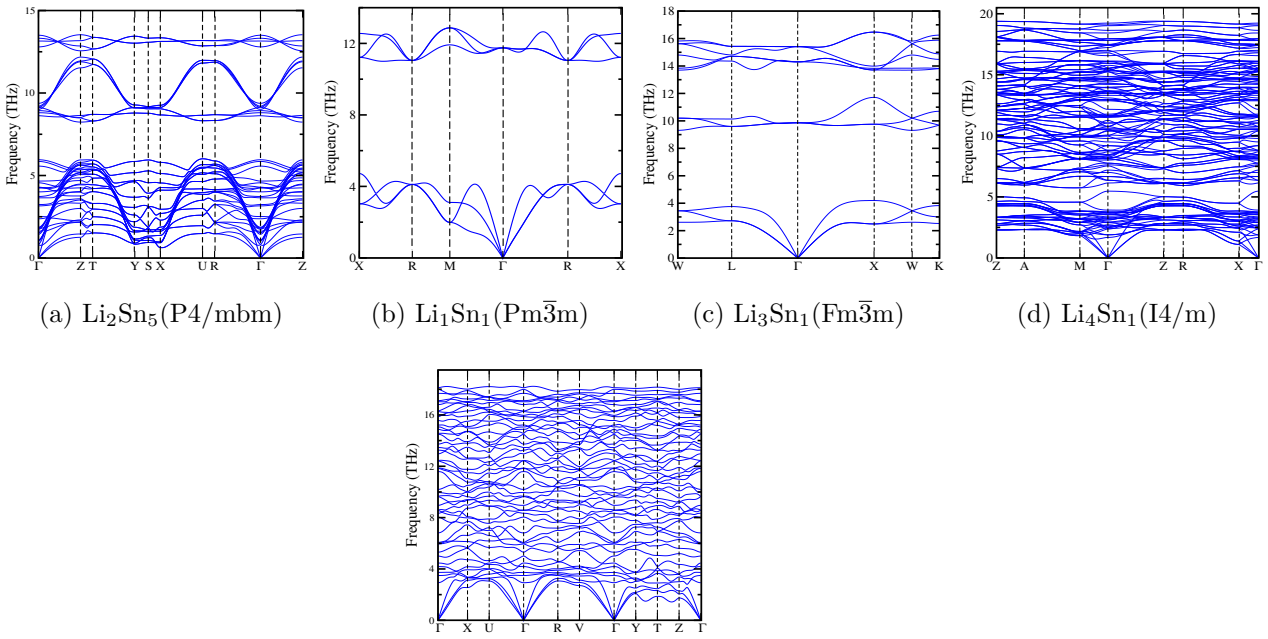

(a) Li_2Sn_5(P4/mbm) (b) Li_1Sn_1(Pm$\bar{3}$m) (c) Li_3Sn_1(Fm$\bar{3}$m) (d) Li_4Sn_1(I4/m)

(e) Li_7Sn_1(P$\bar{1}$)

Figure S2: Phonon dispersion curves of: (a) Li_2Sn_5(P4/mbm), (b) Li_1Sn_1(Pm$\bar{3}$m), (c) Li_3Sn_1(Fm$\bar{3}$m), (d) Li_4Sn_1(I4/m), and (e) Li_7Sn_1(P$\bar{1}$), appeared at 20 GPa convex-hull. Curves are arranged in an increasing order of Li-content.

3. Fitness of selected experimentally identified Li-Sn compounds at 1 atm, 5, 10, and 20 GPa Convexhull

Table T1: Fitness (vertical distance to the convex hull) of selected experimentally identified Li-Sn compounds at 1 atm, 5, 10, and 20 GPa Convex hull. The decomposition energy of these experimentally identified compounds is measured via vertical length from the convex hull tie line.

Stoichiometry	Fitness (eV/atom)			
	P = 1 atm	P = 5 GPa	P = 10 GPa	P = 20 GPa
Li_2Sn_5	0.0027	0.0000	0.0042	0.0315
Li_7Sn_3	0.0013	0.0012	0.0015	0.0028
Li_5Sn_2	0.0020	0.0012	0.0006	0.0000
$Li_{17}Sn_4$	0.0000	0.0000	0.0004	0.0209

4. Formation enthalpies (FEs) of Li-Sn compounds appeared at 1 atm, 5, 10, and 20 GPa convexhull and the contribution of ZPE on the FEs at 1 atm

Table T2: Formation enthalpies (FEs) of Li-Sn compounds appeared at 1 atm, 5, 10, and 20 GPa convexhull and the contribution of ZPE on the FEs at 1 atm pressure.

Stoichiometry	Composition ratio	Formation enthalpy (FE) without ZPE correction (eV/atom)								Contribution of ZPE on the enthalpy of formation at 1 atm pressure
		P = 1 atm		P = 5 GPa		P = 10 GPa		P = 20 GPa		
Li_xSn_y	{y/x+y}	Symmetry	FE (eV/atom)	Symmetry	FE (eV/atom)	Symmetry	FE (eV/atom)	Symmetry	FE (eV/atom)	(meV/atom)
Li_2Sn_5	0.7143	P4/mbm	-0.1844	Pbam	-0.2552	Pbam	-0.2738	Pbam	-0.2985	7.0
Li_1Sn_1	0.5000	P2/m $I4_1/amd$	-0.3273 -0.3208	P2/m	-0.4306	$Pm\bar{3}m$	-0.4865	$Pm\bar{3}m$	-0.5776	-6.0 -6.0
Li_7Sn_3	0.3000	$P2_1/m$	-0.3908	$P2_1/m$	-0.5055	$P2_1/m$	-0.5742	$P2_1/m$	-0.6783	3.0
Li_5Sn_2	0.2857	$R\bar{3}m$	-0.3948	$R\bar{3}m$	-0.5109	$R\bar{3}m$	-0.5814	$R\bar{3}m$	-0.6886	2.0
$Li_{13}Sn_5$	0.2778	$P\bar{3}m1$	-0.3994	$P\bar{3}m1$	-0.5152	$P\bar{3}m1$	-0.5856	$P\bar{3}m1$	-0.6926	3.0
Li_8Sn_3	0.2727	$R\bar{3}m$	-0.3990	$R\bar{3}m$	-0.5148	$R\bar{3}m$	-0.5853	$R\bar{3}m$	-0.6927	3.0
Li_3Sn_1	0.2500	P2/m	-0.3828	$Fm\bar{3}m$	-0.4989	$Fm\bar{3}m$	-0.5696	$Fm\bar{3}m$	-0.6784	3.0
Li_7Sn_2	0.2222	$P\bar{3}m1$ Cmmm	-0.3769 -0.3712	$P\bar{3}m1$	-0.4858	$P\bar{3}m1$	-0.5525	$P\bar{3}m1$	-0.6528	5.0 4.0
Li_4Sn_1	0.2000	$R\bar{3}m$	-0.3443	$R\bar{3}m$	-0.4446	$R\bar{3}m$	-0.5065	I4/m	-0.6086	5.0
$Li_{17}Sn_4$	0.1905	$F\bar{4}3m$	-0.3491	$F\bar{4}3m$	-0.4399	$F\bar{4}3m$	-0.4915	$F\bar{4}3m$	-0.5645	Not Calculated
Li_5Sn_1	0.1667	C2/m	-0.2951	C2/m	-0.3900	C2/m	-0.4466	C2/m	-0.5275	3.0
Li_7Sn_1	0.1250	C2/m	-0.2137	C2/m	-0.2793	C2/m	-0.3204	$P\bar{1}$	-0.4040	6.0

5. Thermodynamic stability of $Li_{17}Sn_4$ at high pressure

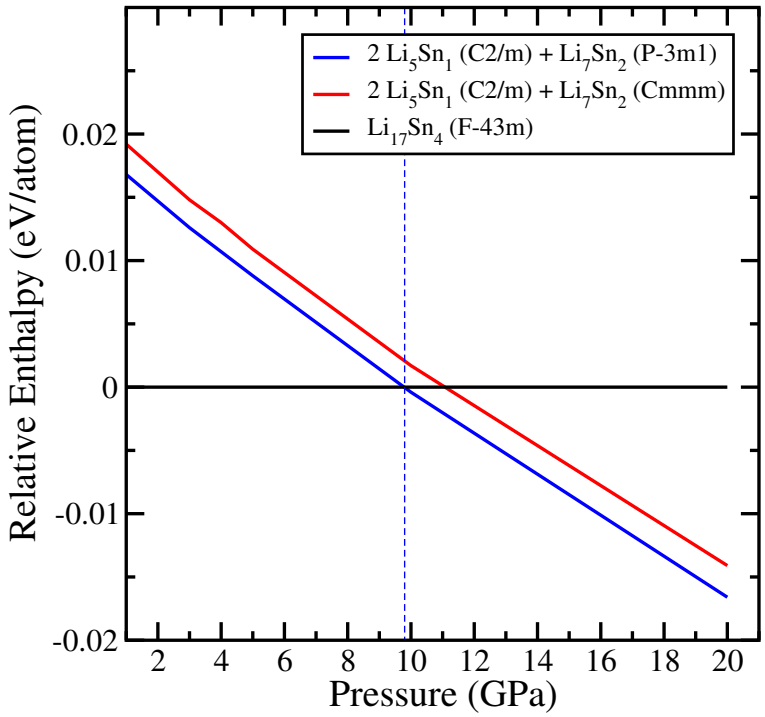

Figure S3: Enthalpies of decomposition of $\mathbf{Li_{17}Sn_4}$ into $\mathbf{Li_5Sn_1}$+ $\mathbf{Li_7Sn_2}$ as a function of pressure.

6. Experimentally known Li-Sn stoichiometries

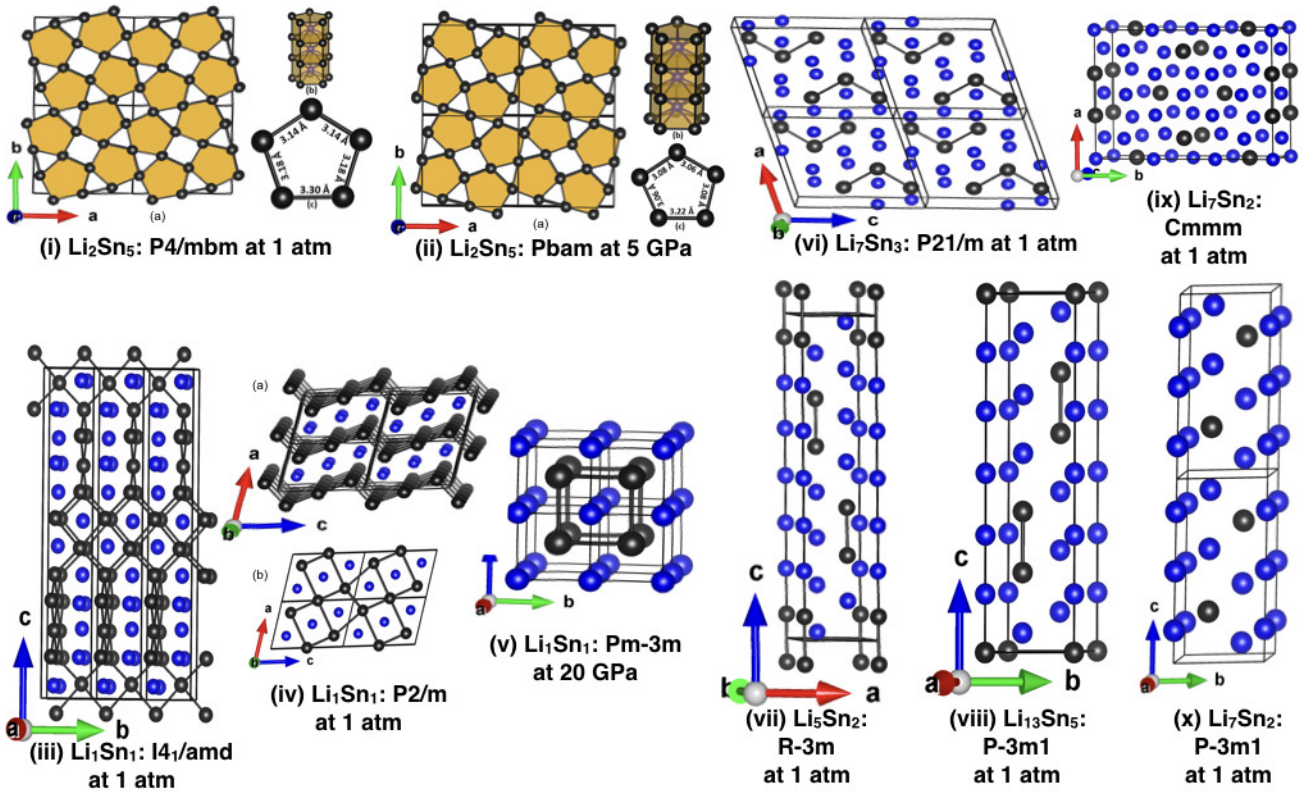

Figure S4: Crystal structures of experimentally known Li-Sn compounds: (i) Li_2Sn_5: P4/mbm at 1atm, (ii) Li_2Sn_5: Pbam at 5 GPa, (iii) Li_1Sn_1: $I4_1/amd$ at 1 atm, (iv) Li_1Sn_1: P2/m at 1 atm, (v) Li_1Sn_1: $Pm\bar{3}m$ at 20 GPa, (vi) Li_7Sn_3: $P2_1/m$ at 1 atm (vii) Li_5Sn_2: $R\bar{3}m$ at 1 atm, (viii) $Li_{13}Sn_5$: $P\bar{3}m1$ at 1 atm, (ix) Li_7Sn_2: Cmmm at 1 atm, and (x) Li_7Sn_2: $P\bar{3}m1$ at 1 atm. Here, blue and black spheres represent Li and Sn atoms, respectively.

a. **Li_2Sn_5:** The Sn-rich Li_2Sn_5 is known to crystallize in the tetragonal system with space group P4/mbm (Figure S4-(i) in SI).[10] Our calculations also predict the same phase to exist till 3.9 GPa, while beyond that P4/mbm structure is found to transform into an orthorhombic structure with space group Pbam (Figure S5 in SI). The P4/mbm - Li_2Sn_5 (with Z = 2) which is isostructural with Mn_2Hg_5, contains pentagonal prisms of Sn with two Li at the extended pole through the center of each prism. This can also be imagined as an infinite number of triangle-quadrangle-pentagon net of Sn atoms in *ab*- plane with Li atoms sandwiched between the two 2D layers of Sn perpendicular to *c* -axis (Figure S4-(i) in SI). While, the high pressure Pbam (with Z = 2) structure is basically the lower symmetry subgroup of the P4/mbm with a = 10.365 Å, b = 9.745 Å, and c = 3.045 Å at 5 GPa pressure (Figure S4-(ii) in SI). At 1 atm pressure, Li-Li, Li-Sn, and Sn-Sn

bond lengths are found to be 3.14 Å, 3.00 Å, and 3.14 Å, respectively, while the respective values get reduced to 2.89 Å, 2.72 Å, and 2.89 Å at 20 GPa pressure.

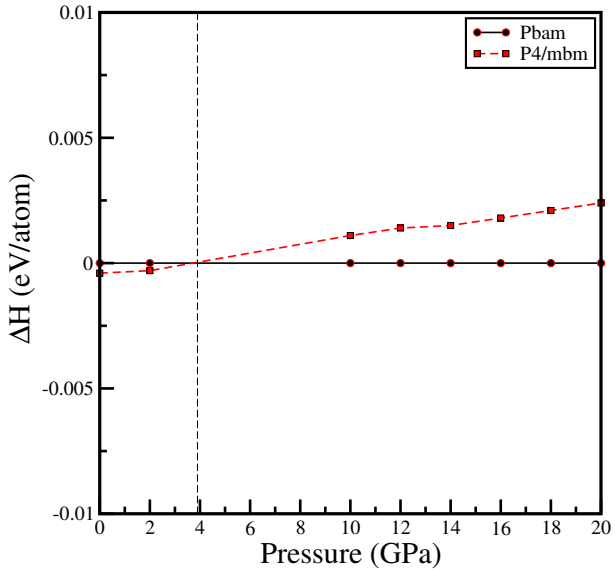

Figure S5: Thermodynamic stability of $\mathbf{Li_2Sn_5}$. Pressure driven **P4/mbm** to **Pbam** phase transition of $\mathbf{Li_2Sn_5}$ is shown.

b. $\mathbf{Li_1Sn_1}$**:** In case of Li_1Sn_1, two types of structures are experimentally reported at ambient pressure: $\alpha - Li_1Sn_1$ which crystallizes in the monoclinic system (space group P2/m, Z = 3, Figure S4-(iv) in SI) and $\beta - Li_1Sn_1$ which belongs to the tetragonal symmetry (space group $I4_1/amd$, Z = 12, Figure S4-(iii) in SI).[11, 12] Our calculations however predict P2/m phase to be energetically more favorable than $I4_1/amd$ by 6 meV/atom at ambient pressure with Li-Li, Li-Sn, and Sn-Sn bond lengths to be 3.11 Å, 3.00 Å, and 3.05 Å, respectively. Interestingly, with the increase in pressure, stability of $\beta - Li_1Sn_1$ further decreases as compared to $\alpha - Li_1Sn_1$. Li_1Sn_1 structure in P2/m phase contains a series of infinite 2D rumpled like surface layers of Sn with Li intercalated in between (Figure S4-(iv)-a in SI). Above, 9 GPa, this phase gets transformed to $Pm\bar{3}m$ with Z=1 (Figure S6 in SI), where the rumpled layers gets converted into 2D flat layers having alternative stacking of Sn and Li atoms (Figure S4-(v) in SI). At 20 GPa, the nearest Li-Li (3.14 Å) and Sn-Sn (3.14 Å) distance remains almost same as in case of P2/m phase at 1 atm pressure, while Li-Sn distance reduces to 2.72 Å.

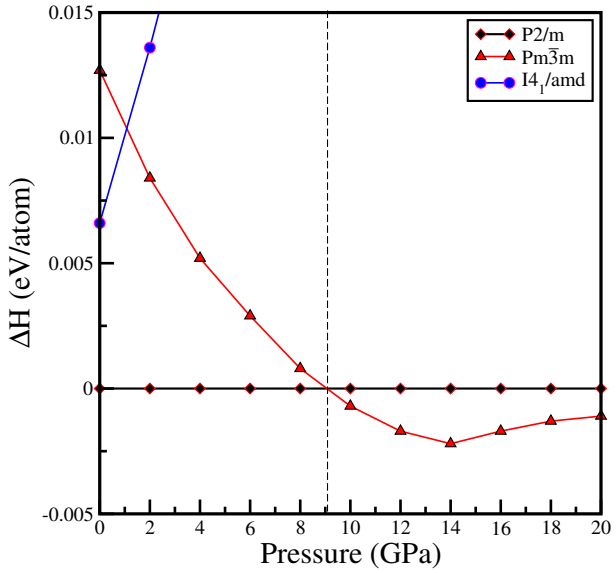

Figure S6: Thermodynamic stability of $\mathbf{Li_1Sn_1}$. Pressure driven $\mathbf{P2/m}$ to $\mathbf{Pm\bar{3}m}$ phase transition of $\mathbf{Li_1Sn_1}$ is shown.

c. **Li_7Sn_3:** It is known that Li_7Sn_3 with monoclinic crystal structure having $P2_1/m$ symmetry (Z=2) can be made by annealing from high-temperature melting and mechanical alloying process.[13] Our calculations also predict the same structure to be the lowest enthalpy structure but, metastable through out the calculated pressure range (situated roughly 1–3 meV/atom above the convex hull, see Table T1 of SI) The structure contains bent trimers of tin atoms with each atomic chain of Sn exclusively surrounded by Li atoms (Figure S4-(vi) in SI). The Li-Li, Li-Sn, and Sn-Sn bond lengths are found to reduce from 2.80 Å, 2.82 Å, and 2.99 Åat 1 atm pressure to 2.48, 2.50, and 2.79 Å at 20 GPa, respectively.

d. **Li_5Sn_2:** For Li_5Sn_2, in agreement with experimental findings[14] we found the trigonal crystal system with $R\bar{3}m$ phase to be most stable. However, our calculations predict this stoichiometry to be thermodynamically metastable at 1 atm pressure which gets stable only above 19 GPa pressure. The structure of Li_5Sn_2 exhibit dumbbells of Sn after every 5 Li atoms in atomic rows, parallel to hexagonal axis. The complete three dimensional structure can be realized by packing these one dimensional linear repeating chains alongside each other (Figure S4-(vii) in SI). It is also noted that the tendency to form Sn-Sn dimers in Li-Sn structures starts from this compositions, which interestingly vanishes when Li occupancy exceeds the value 2.67 per Sn atoms. However, as an exception, Li_7Sn_2 having space group Cmmm (which is not found the stable phase as per our calculations) found to exhibit Sn-Sn isolated dumbbells.[15] The Li-Li, Li-Sn, and Sn-Sn bond lengths in Li_5Sn_2, are found to reduce from 2.79 Å, 2.78 Å, and 2.93

Å at 1 atm pressure to 2.46 Å, 2.47 Å, and 2.75 Å at 20 GPa, respectively.

e. **$Li_{13}Sn_5$:** The crystal structure of $Li_{13}Sn_5$ was first determined by Frank et al.[16] They demonstrated it to crystallize in trigonal structure (space group P$\bar{3}$m1) with 18 atoms per unit cell. Our *ab-initio* evolutionary calculations reveal exactly the same symmetry as the ground state structure of $Li_{13}Sn_5$ with $a = 4.702$ Å and $c/a = 3.644$ at 1 atm pressure. The atomic packing of the structure is very similar to R$\bar{3}$m-Li_5Sn_2 structure, with only a difference that alongside Sn-Sn dimmers, monomers of Sn can also be found in the P$\bar{3}$m1 $-$ $Li_{13}Sn_5$ structure. Thus two different types of linear repeating chains: one with Sn-Sn dimers (dimer length $\sim$ 2.92 Å) after every 5 Li atoms and another having monomer of Sn after every 5 Li atoms with ratio 2:1, are the basic building blocks of the three dimensional structure (Figure S4-(viii) in SI). Moreover, $Li_{13}Sn_5$ is also a perfect example of long range b.c.c superstructure along [1$\bar{1}$0], [01$\bar{1}$], [111] directions where it is easy to observe the rhombic dodecahedron for Li atoms with Sn atom at the center. The minimum Li-Li, Li-Sn, and Sn-Sn bond lengths in $Li_{13}Sn_5$, are found to reduce from 2.81 Å, 2.79 Å, and 2.92 Å at 1 atm pressure to 2.47 Å, 2.48 Å, and 2.75 Å at 20 GPa, respectively.

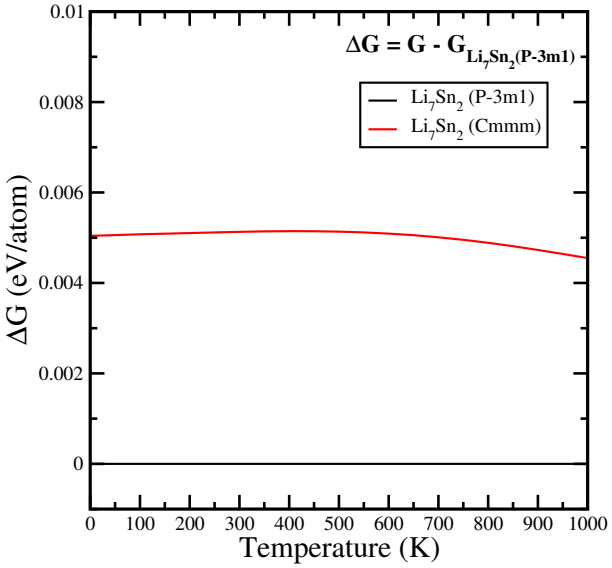

Figure S7: Thermodynamic stability of **Li_7Sn_2**.

f. **Li_7Sn_2:** In case of Li_7Sn_2, experimentally known phase is Cmmm (Z = 4) which reflects Li_7Sn_2 to crystallize in orthorhombic crystal system(Figure S4-(ix)),[15] while our DFT-GGA based calculations predict a more symmetric trigonal crystal system with P$\bar{3}$m1 phase (with Z =1, Figure S4-(x) in SI) to be enthalpically more stable than the experimentally known phase (with structural energy difference, $\triangle$E $\leq$ 6 meV/atom). Such discrepancy was also found in the

study of Genser et. al. for the Li-Sn system,[17] as well as in the study of Morris et. al. for the Li-Ge system.[18] However, keeping in mind that inclusion of zero point energy and lattice vibrational effect due to temperature may alter this discrepancy, we further calculate the Gibbs free energy vs. temperature of both the phases (calculated under quasi-harmonic approximation) at ambient pressure. But no such temperature driven phase transition is observed in between 0 to 1000K in our calculations(Figure S7 in SI). Thus, all the results strongly demand a reinvestigation on Li_7Sn_2 compound. The P$\bar{3}$m1- Li_7Sn_2 phase is found to be isostructural with Li_7Pb_2. The optimized lattice parameters of P$\bar{3}$m1- Li_7Sn_2 phase obtained at ambient pressure are: $a = 4.681$ Å and $c/a = 1.816$, which are about 1–4% higher than reported by Genser et. al.[17] based on the local density approximation (LDA). The atomic arrangement of the P$\bar{3}$m1- Li_7Sn_2 structure is found to be almost same as the structure of Li_5Sn_2 and $Li_{13}Sn_5$, with a difference that Sn-Sn dimers get completely disappeared. The Sn-Sn nearest neighbor distance increases drastically from 2.92 Å in $Li_{13}Sn_5$ to $>$ 4.69 Å in P$\bar{3}$m1- Li_7Sn_2. The trend continues in Li-Sn stoichiometries with higher Li-concentration as well. This is primarily due to the higher Pauling electronegativity of Sn (1.96), which forces all Sn atoms to fulfill the "octet rule" by acquiring a large proportion of charge from highly accessed neighbouring Li atoms and hence, only monomers of Sn exist in Li-rich Sn compounds. Thus, in the complete structure of Li_7Sn_2, two different types of linear repeating chains: one with pure Li atoms and another having monomer of Sn after every 2 Li atoms with ratio 1:2, can be seen (Figure S4-(x) in SI). Similar rows of atoms are also seen in Cmmm- Li_7Sn_2 phase along [110] direction. But, in Cmmm- Li_7Sn_2 structure, the distance between two monomers of Sn in an inter atomic row is 3.21 Å instead of 4.69 Å as observed in P$\bar{3}$m1- Li_7Sn_2 structure (Figure S4-(ix) in SI). The minimum Li-Li, Li-Sn, and Sn-Sn bond lengths in P$\bar{3}$m1-Li_7Sn_2, are found to reduce from 2.73 Å, 2.80Å, and 4.69 Å at 1 atm pressure to 2.38 Å, 2.53 Å, and 4.16 Å at 20 GPa, respectively.

7. Structural parameters

Table T3: Crystal structures of selective Li-Sn compounds at 1 atm pressure and the corresponding atomic Bader charges (Q).

Stoichiometry (Space Group)	Lattice parameters (a, b, and c in Å) (α, β, and γ in degree)	Wyckoff position	X	Y	Z	Q (|e|)	Stoichiometry (Space Group)	Lattice parameters (a, b, and c in Å) (α,β, and γ in degree)	Wyckoff position	X	Y	Z	Q
Li_8Sn_3	a =4.684	Li(6c)	0.00000	0.00000	0.82187	+0.83	**Li_7Sn_1**	a =15.678	Li(4i)	0.03456	0.00000	0.35549	+0.81
($R\bar{3}m$)	c =31.582	Li(6c)	0.00000	0.00000	0.91151	+0.83	(C2/m)	b =4.826	Li(4i)	0.90957	0.00000	0.98930	-0.28
		Li(6c)	0.00000	0.00000	0.36280	+0.83		c =8.058	Li(4i)	0.34529	0.00000	0.78165	-0.05
		Li(6c)	0.00000	0.00000	0.27305	+0.83		β =102.67	Li(4i)	0.59874	0.00000	0.54851	+0.81
		Sn(6c)	0.00000	0.00000	0.54603	-1.96			Li(4i)	0.72394	0.00000	0.90862	+0.82
		Sn(3a)	0.00000	0.00000	0.00000	-2.68			Li(4i)	0.22114	0.00000	0.40170	+0.82
									Li(4i)	0.53519	0.00000	0.83549	+0.81
									Sn(4i)	0.16044	0.00000	0.71642	-3.73
Li_3Sn_1	a =6.885	Li(2m)	0.93728	0.00000	0.19205	+0.83	**Li_8Sn_1**	a =15.918	Li(8j)	0.23212	0.23819	0.37423	+0.81
(P2/m)	b =4.623	Li(2n)	0.16962	0.50000	0.18141	+0.83	(C2/m)	b =5.738	Li(8j)	0.35730	0.24201	0.12869	+0.81
	c =7.060	Li(1h)	0.50000	0.50000	0.50000	+0.83		c =12.043	Li(4i)	0.05996	0.00000	0.38658	+0.81
	β =104.07	Li(2m)	0.26323	0.00000	0.51292	+0.83		β =128.86	Li(8j)	0.97671	0.23903	0.87413	+0.81
		Li(2n)	0.66288	0.50000	0.16051	+0.83			Li(4i)	0.30362	0.00000	0.86329	+0.81
		Sn(2m)	0.38943	0.00000	0.15420	-2.23			Li(8j)	0.40011	0.22485	0.37799	(+0.81/-0.03)
		Sn(1f)	0.00000	0.50000	0.50000	-2.97			Sn(4i)	0.57071	0.00000	0.36776	-3.61
									Sn(4i)	0.18370	0.00000	0.11280	-3.67
Li_7Sn_2	a =4.681	Li(2d)	0.33333	0.66667	0.39716	+0.82	**Li_4Sn_1**	a =4.742	Li(6c)	0.00000	0.00000	0.20553	+0.82
($P\bar{3}m1$)	c =8.501	Li(1b)	0.00000	0.00000	0.50000	+0.82	($R\bar{3}m$)	c =13.932	Li(6c)	0.00000	0.00000	0.60845	+0.82
		Li(2d)	0.33333	0.66667	0.07672	+0.82			Sn(3a)	0.00000	0.00000	0.00000	-3.28
		Li(2c)	0.00000	0.00000	0.17809	+0.82							
		Sn(2d)	0.33333	0.66667	0.73685	-2.88							

Table T4: Crystal structures of selective Li-Sn compounds at 20 GPa and the corresponding atomic Bader charges (Q).

Stoichiometry (Space Group)	Lattice parameters (a, b, and c in Å) (α,β, and γ in degree)	Wyckoff position	X	Y	Z	Q (|e|)	Stoichiometry (Space Group)	Lattice parameters (a, b, c in Å) (α,β, and γ in degree)	Wyckoff position	X	Y	Z	Q (|e|)
Li_2Sn_5	a =10.090	Li(4h)	0.18904	0.65289	0.50000	+0.82	**Li_7Sn_1**	a =4.609	Li(2i)	0.08982	0.94209	0.26804	+0.76
(Pbam)	b =8.955	Sn(4g)	0.05605	0.17532	0.00000	-0.14	($P\bar{1}$)	b =6.693	Li(2i)	0.02194	0.27539	0.94230	-0.79
	c =2.885	Sn(4g)	0.77653	0.09349	0.00000	-0.44		c =6.697	Li(2i)	0.43336	0.28740	0.69773	+0.76
		Sn(2c)	0.00000	0.50000	0.00000	-0.47		α =67.57	Li(2i)	0.70764	0.88964	0.54725	+0.76
								β =79.92	Li(2i)	0.68061	0.59950	0.91842	+0.76
								γ =80.25	Li(2i)	0.20320	0.50876	0.38472	+0.76
									Li(2i)	0.37276	0.91514	0.90975	+0.68
Li_1Sn_1	a =3.135	Li(1a)	0.00000	0.00000	0.00000	+0.81			Sn(2i)	0.22474	0.68709	0.68152	-3.69
($Pm\bar{3}m$)		Sn(1b)	0.50000	0.50000	0.50000	-0.81	**Li_4Sn_1**	a =11.965	Li(8h)	0.38249	0.55903	0.00000	+0.78
							(I4/m)	c =4.241	Li(8h)	0.76672	0.61477	0.00000	+0.78
									Li(8h)	0.04345	0.41742	0.00000	+0.78
									Li(8h)	0.82836	0.80087	0.00000	+0.78
Li_3Sn_1	a =5.867	Li(8c)	0.25000	0.25000	0.25000	+0.80			Li(8h)	0.76776	0.98727	0.00000	+0.78
($Fm\bar{3}m$)		Li(4a)	0.00000	0.00000	0.00000	+0.78			Sn(2b)	0.00000	0.00000	0.00000	-3.38
		Sn(4b)	0.50000	0.50000	0.50000	-2.35			Sn(8h)	0.61033	0.81763	0.00000	-3.04

Table T5: The space group and calculated equilibrium lattice parameters a (Å), b (Å), and c (Å), α(deg), β(deg), γ(deg), and volume (Å^3/atom), at given pressure for Li, Sn and Li-Sn compounds are given. Gravimetric capacities of corresponding Li-Sn compounds are written in first column, in parenthesis.

System (GC) (mAh/g)	Pressure	Space Group (f.u.)	a (Å)	b (Å)	c (Å)	α (°)	β (°)	γ (°)	Volume (Å^3/atom)	System (GC) (mAh/g)	Pressure	Space Group (f.u.)	a (Å)	b (Å)	c (Å)	α (°)	β (°)	γ (°)	Volume (Å^3/atom)
	1 atm	Fd$\bar{3}$m(Z=8)	6.651	6.651	6.651	90.00	90.00	90.00	36.78		1 atm	Im$\bar{3}$m(Z=2)	3.439	3.439	3.439	90.00	90.00	90.00	20.33
Sn	5 GPa	I4$_1$/amd(Z=4)	5.948	5.948	3.201	90.00	90.00	90.00	28.31	**Li**	5 GPa	Im$\bar{3}$m(Z=2)	3.175	3.175	3.175	90.00	90.00	90.00	16.00
(-)	10 GPa	I4/mmm(Z=2)	3.778	3.778	3.349	90.00	90.00	90.00	23.91	**(-)**	10 GPa	Fm$\bar{3}$m(Z=4)	3.814	3.814	3.814	90.00	90.00	90.00	13.87
	20 GPa	I4/mmm(Z=2)	3.647	3.647	3.285	90.00	90.00	90.00	21.84		20 GPa	Fm$\bar{3}$m(Z=4)	3.591	3.591	3.591	90.00	90.00	90.00	11.57
	1 atm	P4/mbm(Z=2)	10.378	10.378	3.141	90.00	90.00	90.00	24.17		1 atm	C2/m(Z=4)	15.678	4.826	8.058	90.00	102.67	90.00	18.59
Li$_2$Sn$_5$	5 GPa	Pbam(Z=2)	10.365	9.745	3.045	90.00	90.00	90.00	21.97	**Li$_7$Sn$_1$**	5 GPa	C2/m(Z=4)	14.762	4.556	7.598	90.00	102.40	90.00	15.60
(90)	10 GPa	Pbam(Z=2)	10.247	9.407	2.981	90.00	90.00	90.00	20.52	**(1580)**	10 GPa	C2/m(Z=4)	14.208	4.392	7.324	90.00	102.14	90.00	13.96
	20 GPa	Pbam(Z=2)	10.090	8.955	2.885	90.00	90.00	90.00	18.62		20 GPa	P$\bar{1}$(Z=2)	4.609	6.693	6.697	67.57	79.92	80.25	11.68
	1 atm	P2/m(Z=3)	5.178	3.225	7.812	90.00	105.25	90.00	20.98		1 atm	C2/m(Z=8)	15.918	5.738	12.043	90.00	128.86	90.00	17.84
		I4$_1$/amd(Z=12)	4.454	4.454	26.043	90.00	90.00	90.00	21.53										
Li$_1$Sn$_1$	5 GPa	P2/m(Z=3)	4.940	3.145	7.526	90.00	106.18	90.00	18.72	**Li$_5$Sn$_1$**	5 GPa	C2/m(Z=8)	15.135	5.474	11.453	90.00	128.87	90.00	15.39
(226)	10 GPa	Pm$\bar{3}$m(Z=1)	3.248	3.248	3.248	90.00	90.00	90.00	17.14	**(1129)**	10 GPa	C2/m(Z=8)	14.631	5.308	11.076	90.00	128.83	90.00	13.96
	20 GPa	Pm$\bar{3}$m(Z=1)	3.135	3.135	3.135	90.00	90.00	90.00	15.41		20 GPa	C2/m(Z=8)	13.948	5.089	10.568	90.00	128.71	90.00	12.20
	1 atm	P2$_1$/m(Z=2)	8.562	4.738	9.491	90.00	106.10	90.00	18.50		1 atm	F4$\bar{3}$m(Z=20)	19.714	19.714	19.714	90.00	90.00	90.00	18.24
Li$_7$Sn$_3$	5 GPa	P2$_1$/m(Z=2)	8.225	4.528	9.092	90.00	106.07	90.00	16.27	**Li$_{17}$Sn$_4$**	5 GPa	F4$\bar{3}$m(Z=20)	18.789	18.789	18.789	90.00	90.00	90.00	15.79
(527)	10 GPa	P2$_1$/m(Z=2)	8.009	4.387	8.341	90.00	106.05	90.00	14.91	**(960)**	10 GPa	F4$\bar{3}$m(Z=20)	18.198	18.198	18.198	90.00	90.00	90.00	14.35
	20 GPa	P2$_1$/m(z=2)	7.710	4.196	8.489	90.00	106.03	90.00	13.20		20 GPa	F4$\bar{3}$m(Z=20)	17.398	17.398	17.398	90.00	90.00	90.00	12.54
	1 atm	R$\bar{3}$m(Z=3)	4.732	4.732	19.810	90.00	90.00	120.00	18.29		1 atm	R$\bar{3}$m(Z=3)	4.742	4.742	13.932	90.00	90.00	120.00	18.08
Li$_5$Sn$_2$	5 GPa	R$\bar{3}$m(Z=3)	4.520	4.520	19.079	90.00	90.00	120.00	16.07	**Li$_4$Sn$_1$**	5 GPa	R$\bar{3}$m(Z=3)	4.524	4.524	13.173	90.00	90.00	120.00	15.57
(564)	10 GPa	R$\bar{3}$m(Z=3)	4.376	4.376	18.629	90.00	90.00	120.00	14.72	**(903)**	10 GPa	R$\bar{3}$m(Z=3)	4.386	4.386	12.701	90.00	90.00	120.00	14.11
	20 GPa	R$\bar{3}$m(Z=3)	4.187	4.187	17.994	90.00	90.00	120.00	13.01		20 GPa	I4/m(Z=10)	11.965	11.965	4.241	90.00	90.00	90.00	12.14
	1 atm	P$\bar{3}$m1(Z=1)	4.702	4.702	17.133	90.00	90.00	120.00	18.23		1 atm	P$\bar{3}$m1(Z=1)	4.681	4.681	8.501	90.00	90.00	120.00	17.93
												Cmmm(Z=4)	9.812	13.887	4.728	90.00	90.00	90.00	17.90
Li$_{13}$Sn$_5$	5 GPa	P$\bar{3}$m1(Z=1)	4.495	4.495	16.458	90.00	90.00	120.00	16.00	**Li$_7$Sn$_2$**	5 GPa	P$\bar{3}$m1(Z=1)	4.476	4.476	8.088	90.00	90.00	120.00	15.59
(587)	10 GPa	P$\bar{3}$m1(Z=1)	4.358	4.358	16.020	90.00	90.00	120.00	14.64	**(790)**	10 GPa	P$\bar{3}$m1(Z=1)	4.341	4.341	7.828	90.00	90.00	120.00	14.20
	20 GPa	P$\bar{3}$m1(Z=1)	4.173	4.173	15.433	90.00	90.00	120.00	12.93		20 GPa	P$\bar{3}$m1(Z=1)	4.160	4.160	7.485	90.00	90.00	120.00	12.46
	1 atm	R$\bar{3}$m(Z=3)	4.684	4.684	31.582	90.00	90.00	120.00	18.18		1 atm	P2/m(Z=3)	6.885	4.623	7.060	90.00	104.07	90.00	18.16
Li$_8$Sn$_3$	5 GPa	R$\bar{3}$m(Z=3)	4.478	4.478	30.298	90.00	90.00	120.00	15.94	**Li$_3$Sn$_1$**	5 GPa	Fm$\bar{3}$m(Z=4)	6.305	6.305	6.305	90.00	90.00	90.00	15.67
(602)	10 GPa	R$\bar{3}$m(Z=3)	4.343	4.343	29.462	90.00	90.00	120.00	14.58	**(677)**	10 GPa	Fm$\bar{3}$m(Z=4)	6.119	6.119	6.119	90.00	90.00	90.00	14.32
	20 GPa	R$\bar{3}$m(Z=3)	4.161	4.161	28.337	9000	90.00	120.00	12.87		20 GPa	Fm$\bar{3}$m(Z=4)	5.867	5.867	5.867	90.00	90.00	90.00	12.62

8. Shortest interatomic distance for Li-Sn compounds

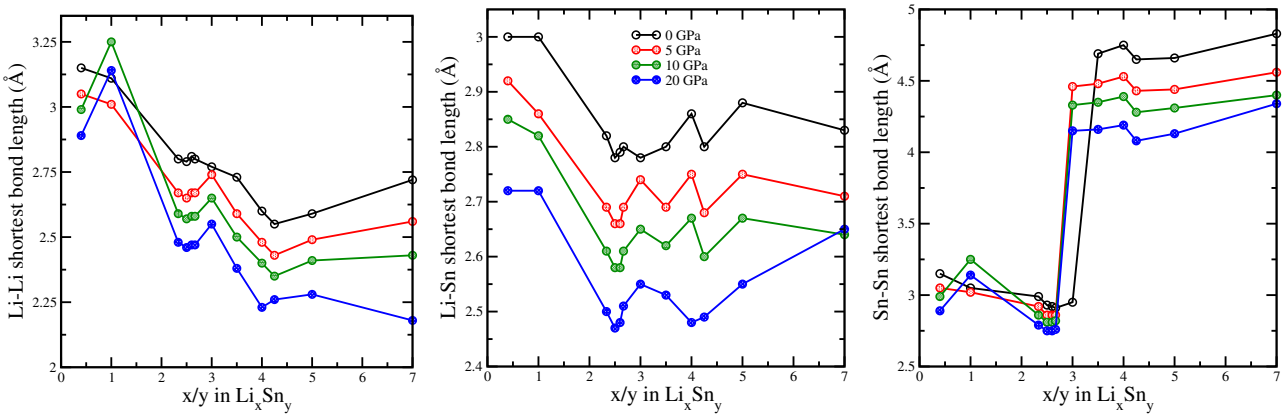

(a) (b) (c)

Figure S8: The shortest: (a) Li-Li, (b) Li-Sn, and (c) Sn-Sn, distance for Li-Sn compounds at 1 atm, 5GPa, 10GPa, and 20 GPa pressure.

Table T6: The shortest Li-Li, Li-Sn, and Sn-Sn distance for Li-Sn compounds at 1 atm, 5GPa, 10GPa, and 20 GPa pressure.

Stoichiometry	The shortest atom-atom distance for Li-Sn compounds. (Å)															
	P = 1 atm				P = 5 GPa				P = 10 GPa				P = 20 GPa			
Li_xSn_y	Symmetry	Li-Li	Li-Sn	Sn-Sn	Symmetry	Li-Li	Li-Sn	Sn-Sn	Symmetry	Li-Li	Li-Sn	Sn-Sn	Symmetry	Li-Li	Li-Sn	Sn-Sn
Li_2Sn_5	P4/mbm	3.14	3.00	3.14	Pbam	3.05	2.92	3.05	Pbam	2.99	2.85	2.99	Pbam	2.89	2.72	2.89
Li_1Sn_1	P2/m $I4_1/amd$	3.11 2.99	3.00 3.06	3.05 3.06	P2/m	3.01	2.86	3.02	$Pm\bar{3}m$	3.25	2.82	3.25	$Pm\bar{3}m$	3.14	272	3.14
Li_7Sn_3	$P2_1/m$	2.80	2.82	2.99	$P2_1/m$	2.67	2.69	2.92	$P2_1/m$	2.59	2.61	2.86	$P2_1/m$	2.48	2.50	2.79
Li_5Sn_2	$R\bar{3}m$	2.79	2.78	2.93	$R\bar{3}m$	2.65	2.66	2.86	$R\bar{3}m$	2.57	2.58	2.81	$R\bar{3}m$	2.46	2.47	2.75
$Li_{13}Sn_5$	$P\bar{3}m1$	2.81	2.79	2.92	$P\bar{3}m1$	2.67	2.66	2.86	$P\bar{3}m1$	2.58	2.58	2.81	$P\bar{3}m1$	2.47	2.48	2.75
Li_8Sn_3	$R\bar{3}m$	2.80	2.80	2.91	$R\bar{3}m$	2.67	2.69	2.86	$R\bar{3}m$	2.58	2.61	2.82	$R\bar{3}m$	2.47	2.51	2.76
Li_3Sn_1	P2/m	2.77	2.78	2.95	$Fm\bar{3}m$	2.74	2.74	4.46	$Fm\bar{3}m$	2.65	2.65	4.33	$Fm\bar{3}m$	2.55	2.55	4.15
Li_7Sn_2	$P\bar{3}m1$ Cmmm	2.73 2.70	2.80 2.84	4.69 3.21	$P\bar{3}m1$	2.59	2.69	4.48	$P\bar{3}m1$	2.50	2.62	4.35	$P\bar{3}m1$	2.38	2.53	4.16
Li_4Sn_1	$R\bar{3}m$	2.60	2.86	4.75	$R\bar{3}m$	2.48	2.75	4.53	$R\bar{3}m$	2.40	2.67	4.39	I4/m	2.23	2.48	4.19
$Li_{17}Sn_4$	$F\bar{4}3m$	2.55	2.80	4.65	$F\bar{4}3m$	2.43	2.68	4.43	$F\bar{4}3m$	2.35	2.60	4.28	$F\bar{4}3m$	2.26	2.49	4.08
Li_5Sn_1	C2/m	2.59	2.88	4.66	C2/m	2.49	2.75	4.44	C2/m	2.41	2.67	4.31	C2/m	2.28	2.55	4.13
Li_7Sn_1	C2/m	2.72	2.83	4.83	C2/m	2.56	2.71	4.56	C2/m	2.43	2.64	4.40	$P\bar{1}$	2.18	2.65	4.34

9. Thermodynamic stability of Li_3Sn_1

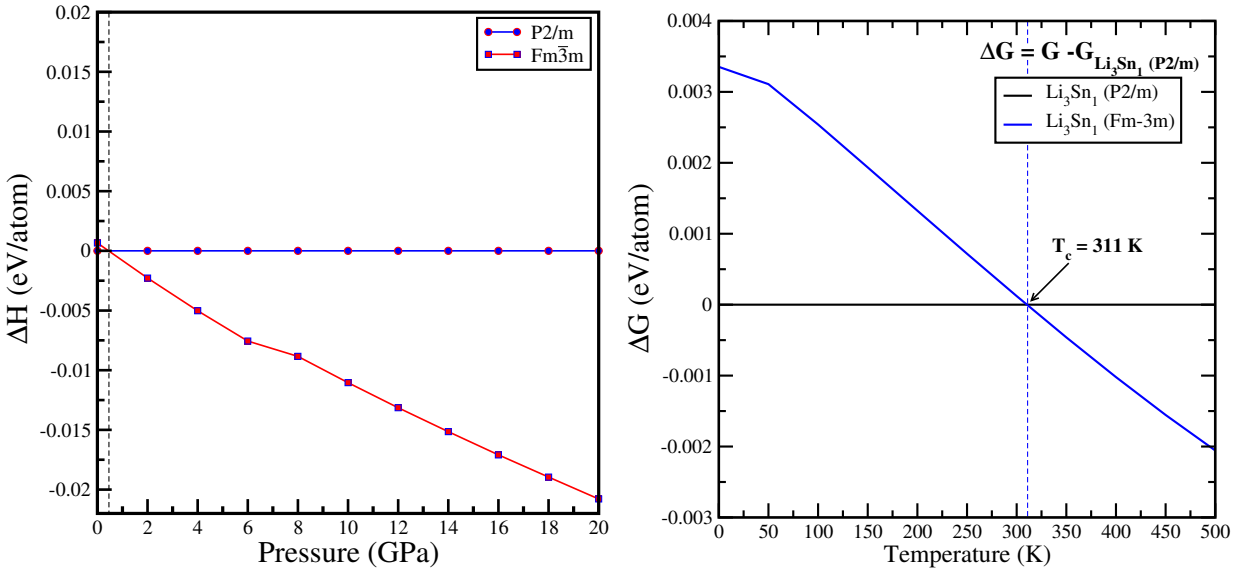

(a) (b)

Figure S9: Thermodynamic stability of $\mathbf{Li_3Sn_1}$. (a) Pressure driven $\mathbf{P2/m}$ to $\mathbf{Pm\bar{3}m}$ phase transition of $\mathbf{Li_3Sn_1}$, (b) Temperature driven $\mathbf{P2/m}$ to $\mathbf{Pm\bar{3}m}$ phase transition of $\mathbf{Li_3Sn_1}$ is shown.

10. Thermodynamic stability of Li_4Sn_1

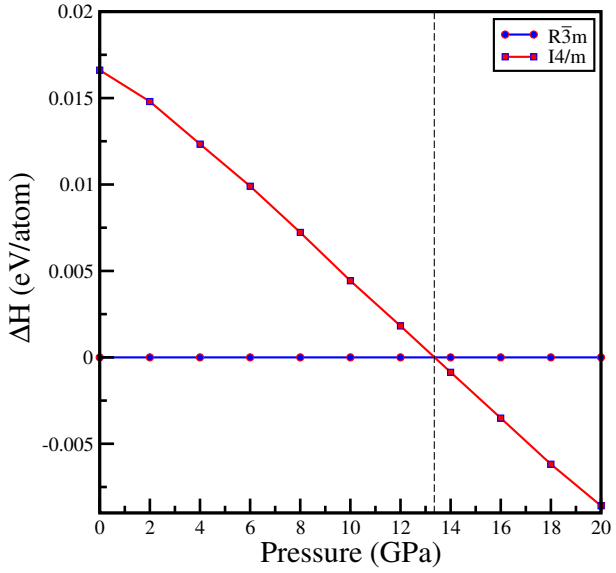

Figure S10: Thermodynamic stability of $\mathbf{Li_4Sn_1}$. Pressure driven $\mathbf{R\bar{3}m}$ to $\mathbf{I4/m}$ phase transition of $\mathbf{Li_4Sn_1}$ is shown.

11. Thermodynamic stability of Li_7Sn_1

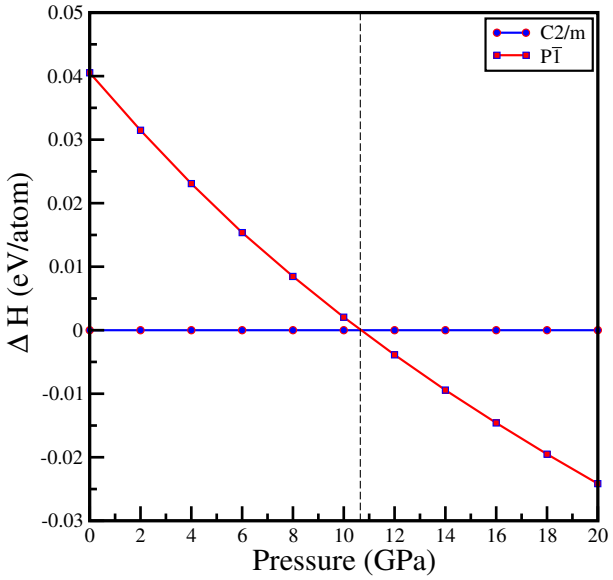

Figure S11: Thermodynamic stability of $\mathbf{Li_7Sn_1}$. Pressure driven $\mathbf{C2/m}$ to $\mathbf{P\bar{1}}$ phase transition of $\mathbf{Li_7Sn_1}$ is shown.

12. Mechanical properties of Li-Sn compounds

The continuum model based on Reuss and Voigt approaches are explicitly used for studies of B_R, B_V and G_R, G_V which are respectively the bulk modulus and shear modulus from the Reuss and Voigt approximations, can be expressed by the following equations:

$$B_R = [S_{11} + S_{22} + S_{33} + 2(S_{12} + S_{13} + S_{23})]^{-1} \quad (3)$$

$$B_V = \frac{1}{9}[C_{11} + C_{22} + C_{33} - 2(C_{12} + C_{13} + C_{23})] \quad (4)$$

$$G_R = 15[4(S_{11} + S_{22} + S_{33}) - 4(S_{12} + S_{13} + S_{23}) + 3(S_{44} + S_{55} + S_{66})]^{-1} \quad (5)$$

$$G_V = \frac{1}{15}[C_{11} + C_{22} + C_{33} - (C_{12} + C_{13} + C_{23}) + 3(C_{44} + C_{55} + C_{66})] \quad (6)$$

where, S_{ij} and C_{ij} are the single crystal elastic compliance constants and elastic stiffness constants, respectively.

Hill has proved that actual elastic moduli for polycrystals can be approximated from the arithmetic mean of Voigt and Reuss moduli which basically represent the

upper and lower limits of the true polycrystalline constants. We therefore move towards the Voigt-Reuss-Hill approximation[8] and express the bulk and shear modulus as follows:

$$B = \frac{1}{2}(B_V + B_R) \tag{7}$$

$$G = \frac{1}{2}(G_V + G_R) \tag{8}$$

After getting the value of B and G, Young's modulus (E) and Poisson's ratio (ν) can easily be determined using the following formula:

$$E = \frac{9BG}{3B + G} \tag{9}$$

$$\nu = \frac{3B-2G}{2(3B + G)} \tag{10}$$

1. **Elastic Constants of Li-Sn compounds.**

Table T7: Elastic constants C_{ij} for Li, Sn, and Li-Sn compounds at 1 atm, where all quantities are in units of GPa.

Elements	Sn	Li_2Sn_5	Li_1Sn_1		Li_7Sn_3	Li_5Sn_2	$Li_{13}Sn_5$	Li_8Sn_3	Li_3Sn_1	Li_7Sn_2		Li_4Sn_1	Li_7Sn_1	Li_5Sn_1	Li
Space group	$Fd\bar{3}m$	P4/mbm	P2/m	$I4_1/amd$	$P2_1/m$	$R\bar{3}m$	$P\bar{3}m1$	$R\bar{3}m$	P2/m	$P\bar{3}m1$	Cmmm	$R\bar{3}m$	C2/m	C2/m	$Im\bar{3}m$
C_{ij}															
C_{11}	56.12	79.03	65.99	63.88	61.44	73.02	75.52	72.51	43.11	69.69	55.05	73.59	56.62	58.33	15.09
C_{22}			80.53		77.07				67.09		68.80		52.74	65.85	
C_{33}		95.24	64.46	65.53	82.62	103.20	110.90	106.72	68.17	80.55	77.40	75.37	51.67	45.84	
C_{44}	43.26	19.85	15.64	28.13	8.94	17.65	20.03	21.44	15.41	18.38	12.21	8.40	27.01	16.74	7.26
C_{55}			18.25		36.99				46.96		33.82		27.84	19.63	
C_{66}		14.93	16.17	5.30	36.25				37.16		39.75		21.15	7.35	
C_{12}	26.60	37.11	12.50	20.29	18.38	11.13	13.57	15.12	20.71	16.10	19.72	9.19	9.14	-5.87	13.38
C_{13}		15.45	29.89	26.55	19.25	2.68	-2.29	-1.29	25.80	0.57	14.69	0.60	11.85	12.71	
C_{14}						12.49	13.59	-14.23		10.07		-9.28			
C_{15}			2.65		-14.08				-5.32				-3.94	1.41	
C_{23}			20.59		-5.88				-1.43		-6.05		13.31	6.65	
C_{25}			-2.39		7.43				-0.68				-2.82	6.22	
C_{35}			-0.22		9.06				-1.78				7.83	-8.10	
C_{46}			-0.48		8.28				-2.17				-4.06	8.22	

Table T8: Elastic constants C_{ij} for Li, Sn, and Li-Sn compounds at 5 GPa, where all quantities are in units of GPa.

Elements	Sn	Li_2Sn_5	Li_1Sn_1	Li_7Sn_3	Li_5Sn_2	$Li_{13}Sn_5$	Li_8Sn_3	Li_3Sn_1	Li_7Sn_2	Li_4Sn_1	Li_7Sn_1	Li_5Sn_1	Li
Space group	$I4_1/amd$	Pbam	P2/m	$P2_1/m$	$R\bar{3}m$	$P\bar{3}m1$	$R\bar{3}m$	$Fm\bar{3}m$	$P\bar{3}m1$	$R\bar{3}m$	C2/m	C2/m	$Im\bar{3}m$
C_{ij}													
C_{11}	136.47	108.11	94.03	85.02	102.99	105.14	102.43	63.86	100.06	105.00	90.56	84.47	26.68
C_{22}		102.94	115.87	104.56							96.23	96.99	
C_{33}	128.01	129.68	95.62	121.81	154.48	155.03	145.43		111.01	109.93	86.07	71.41	
C_{44}	28.44	23.84	27.09	16.30	27.50	28.86	30.34	50.86	24.59	8.84	29.37	23.14	24.13
C_{55}		25.79	28.64	52.58							35.29	28.17	
C_{66}	17.06	29.78	27.56	50.07							29.91	12.72	
C_{12}	24.19	49.15	24.54	31.71	19.60	23.14	23.91	33.78	23.63	18.60	12.53	-2.30	23.10
C_{13}	38.90	25.24	36.39	28.37	5.96	1.44	3.71		7.05	4.77	14.88	23.42	
C_{14}					16.68	18.22	-18.50		13.21	-12.31			
C_{15}			-0.51	-20.57							2.93	1.51	
C_{23}		27.22	30.55	-3.19							16.57	13.14	
C_{25}			0.90	9.81							3.20	7.67	
C_{35}			2.54	10.94							-6.16	-7.91	
C_{46}			-0.18	10.56							1.85	11.32	

Table T9: Elastic constants C_{ij} for Li, Sn, and Li-Sn compounds at 10 GPa, where all quantities are in units of GPa.

Elements	Sn	Li_2Sn_5	Li_1Sn_1	Li_7Sn_3	Li_5Sn_2	$Li_{13}Sn_5$	Li_8Sn_3	Li_3Sn_1	Li_7Sn_2	Li_4Sn_1	Li_7Sn_1	Li_5Sn_1	Li
Space group	I4/mmm	Pbam	$Pm\bar{3}m$	$P2_1/m$	$R\bar{3}m$	$P\bar{3}m1$	$R\bar{3}m$	$Fm\bar{3}m$	$P\bar{3}m1$	$R\bar{3}m$	C2/m	C2/m	$Fm\bar{3}m$
C_{ij}													
C_{11}	91.87	132.32	87.84	103.81	122.60	129.33	125.42	74.30	124.40	129.67	112.39	116.65	38.92
C_{22}		137.88		125.38							117.74	100.24	
C_{33}	108.56	173.33		148.21	177.95	187.43	175.10		138.07	135.16	105.51	88.10	
C_{44}	22.84	27.78	43.50	20.46	34.65	36.28	36.91	60.04	30.50	11.59	35.74	35.07	13.96
C_{55}		29.71		62.87							42.01	29.21	
C_{66}	47.00	33.19		59.55							36.81	15.99	
C_{12}	74.43	61.72	56.54	39.88	25.15	30.18	30.88	44.12	31.27	25.45	19.65	2.32	30.93
C_{13}	75.94	28.14		35.55	12.24	6.08	9.50		11.48	9.75	20.94	17.80	
C_{14}					19.89	21.94	-22.44		15.09	-13.68			
C_{15}				24.17							3.57	-2.77	
C_{23}		29.90		-1.60							24.88	31.51	
C_{25}				-11.83							3.97	2.03	
C_{35}				-12.09							-8.06	1.01	
C_{46}				-12.44							1.91	1.09	

Table T10: Elastic constants C_{ij} for Li, Sn, and Li-Sn compounds at 20 GPa, where all quantities are in units of GPa.

Elements	Sn	Li_2Sn_5	Li_1Sn_1	Li_7Sn_3	Li_5Sn_2	$Li_{13}Sn_5$	Li_8Sn_3	Li_3Sn_1	Li_7Sn_2	Li_4Sn_1	Li_7Sn_1	Li_5Sn_1	Li
Space group	I4/mmm	Pbam	$Pm\bar{3}m$	$P2_1/m$	$R\bar{3}m$	$P\bar{3}m1$	$R\bar{3}m$	$Fm\bar{3}m$	$P\bar{3}m1$	I4/m	C2/m	$P\bar{1}$	$Fm\bar{3}m$
C_{ij}													
C_{11}	136.61	182.52	125.83	141.97	164.34	166.65	161.74	101.72	163.71	164.88	155.79	136.58	56.84
C_{22}		192.01		166.79							163.90	123.70	
C_{33}	143.10	228.71		201.32	239.79	236.91	221.78		181.44	184.76	150.01	114.85	
C_{44}	45.16	35.11	59.24	29.73	47.08	47.86	47.77	76.81	40.09	58.37	57.32	53.58	14.02
C_{55}		35.79		82.78							57.85	45.55	
C_{66}	71.42	40.56		78.94						33.65	43.40	48.02	
C_{12}	97.25	75.59	76.56	57.24	39.46	42.57	45.54	63.28	43.53	22.99	18.42	26.17	46.90
C_{13}	105.69	47.66		49.98	19.90	15.26	18.27		18.83	26.12	35.43	38.15	
C_{14}					25.61	27.68	28.75		18.20			2.96	
C_{15}				-30.63							-2.05	2.76	
C_{16}										-11.02		6.81	
C_{23}		48.01		3.45							32.32	45.57	
C_{24}												4.23	
C_{25}				15.55							-2.36	-2.57	
C_{26}												1.04	
C_{34}												-4.65	
C_{35}				14.49							6.41	-0.14	
C_{36}												-5.27	
C_{45}												-0.01	
C_{46}				16.04							1.94	-0.89	
C_{56}												5.20	

2. **Calculated shear modulus (G), bulk modulus (B), Young's modulus (Y) and Poisson's ratio (ν) for Li, Sn, and Li-Sn compounds**

Table T11: Shear modulus (G), Bulk modulus (B), Young's modulus (Y) and Poisson's ratio (ν) for Li, Sn, and Li-Sn compounds at 1 atm. Except for ν, all quantities are in units of GPa.

Elements		Sn	Li_2Sn_5	Li_1Sn_1		Li_7Sn_3	Li_5Sn_2	$Li_{13}Sn_5$	Li_8Sn_3	Li_3Sn_1	Li_7Sn_2		Li_4Sn_1	Li_7Sn_1	Li_5Sn_1	Li
Space group		$Fd\bar{3}m$	P4/mbm	P2/m	$I4_1/amd$	$P2_1/m$	$R\bar{3}m$	$P\bar{3}m1$	$R\bar{3}m$	P2/m	$P\bar{3}m1$	Cmmm	$R\bar{3}m$	C2/m	C2/m	$Im\bar{3}m$
B	This work	36.44	43.24	37.40	37.72	31.53	31.17	30.97	30.64	29.75	28.26	28.63	27.01	25.51	21.89	13.95
	Other source[#] [19]		45.21	36.43		30.28	29.72	29.34				27.30				14.06
G	This work	28.13	22.06	19.16	17.08	22.90	23.61	25.42	24.65	24.55	22.90	25.80	17.33	22.91	13.85	3.26
	Other source[#] [19]		30.62	18.35		25.25	27.86	29.72				24.13				5.41
Y	This work	67.13	56.56	49.09	44.52	55.31	56.56	59.87	58.31	57.77	54.08	59.51	42.83	52.89	34.31	9.07
	Other source[#] [19]		75.00	47.24		59.53	63.26	65.68				55.43				14.37
ν	This work	0.19	0.28	0.28	0.30	0.21	0.20	0.18	0.18	0.18	0.18	0.15	0.24	0.15	0.24	0.39
	Other source[#] [19]		0.22	0.28		0.17	0.15	0.13				0.16				0.33

[#] Values are extracted from the figures in ref.[19]

Table T12: Shear modulus (G), Bulk modulus (B), Young's modulus (Y) and Poisson's ratio (ν) for Li, Sn, and Li-Sn compounds at 5 GPa. Except for ν, all quantities are in units of GPa.

Elements	Sn	Li_2Sn_5	Li_1Sn_1	Li_7Sn_3	Li_5Sn_2	$Li_{13}Sn_5$	Li_8Sn_3	Li_3Sn_1	Li_7Sn_2	Li_4Sn_1	Li_7Sn_1	Li_5Sn_1	Li
Space group	$I4_1/amd$	Pbam	P2/m	$P2_1/m$	$R\bar{3}m$	$P\bar{3}m1$	$R\bar{3}m$	$Fm\bar{3}m$	$P\bar{3}m1$	$R\bar{3}m$	C2/m	C2/m	$Im\bar{3}m$
B	67.20	60.43	54.17	47.16	46.67	46.17	45.74	43.81	42.94	41.77	40.06	35.70	24.29
G	32.09	30.68	30.48	33.87	34.97	35.22	34.59	31.29	31.51	21.13	33.75	21.57	9.61
Y	83.04	78.72	77.00	81.98	83.95	84.23	82.89	75.82	75.95	54.24	79.05	53.85	25.47
ν	0.29	0.28	0.26	0.21	0.20	0.20	0.20	0.21	0.21	0.28	0.17	0.25	0.32

Table T13: Shear modulus (G), Bulk modulus (B), Young's modulus (Y) and Poisson's ratio (ν) for Li, Sn, and Li-Sn compounds at 10 GPa. Except for ν, all quantities are in units of GPa.

Elements	Sn	Li_2Sn_5	Li_1Sn_1	Li_7Sn_3	Li_5Sn_2	$Li_{13}Sn_5$	Li_8Sn_3	Li_3Sn_1	Li_7Sn_2	Li_4Sn_1	Li_7Sn_1	Li_5Sn_1	Li
Space group	I4/mmm	Pbam	$Pm\bar{3}m$	$P2_1/m$	$R\bar{3}m$	$P\bar{3}m1$	$R\bar{3}m$	$Fm\bar{3}m$	$P\bar{3}m1$	$R\bar{3}m$	C2/m	C2/m	$Fm\bar{3}m$
B	82.31	75.87	66.97	58.23	57.61	58.72	58.22	54.18	55.03	53.79	51.80	45.36	33.59
G	19.81	37.58	28.89	41.00	41.81	43.25	41.48	34.73	39.11	26.96	40.46	30.54	8.48
Y	55.02	96.76	75.76	99.62	101.00	104.17	100.55	85.84	94.86	69.31	96.31	74.84	23.47
ν	0.39	0.29	0.31	0.21	0.21	0.20	0.21	0.24	0.21	0.29	0.19	0.23	0.38

Table T14: Shear modulus (G), Bulk modulus (B), Young's modulus (Y) and Poisson's ratio (ν) for Li, Sn, and Li-Sn compounds at 20 GPa. Except for ν, all quantities are in units of GPa.

Elements	Sn	Li_2Sn_5	Li_1Sn_1	Li_7Sn_3	Li_5Sn_2	$Li_{13}Sn_5$	Li_8Sn_3	Li_3Sn_1	Li_7Sn_2	Li_4Sn_1	Li_7Sn_1	Li_5Sn_1	Li
Space group	I4/mmm	Pbam	$Pm\bar{3}m$	$P2_1/m$	$R\bar{3}m$	$P\bar{3}m1$	$R\bar{3}m$	$Fm\bar{3}m$	$P\bar{3}m1$	I4/m	C2/m	$P\bar{1}$	$Fm\bar{3}m$
B	114.59	105.02	92.98	81.10	80.20	79.27	78.62	76.09	74.57	73.76	71.32	66.08	50.21
G	34.38	48.20	41.66	55.61	55.55	55.18	51.80	44.36	51.31	56.36	56.49	46.15	9.26
Y	93.76	125.41	108.75	135.80	135.40	134.36	127.41	111.42	125.21	134.75	134.06	112.30	26.16
ν	0.36	0.30	0.31	0.22	0.22	0.22	0.23	0.26	0.22	0.20	0.19	0.22	0.41

13. Total and local DOS of Li-Sn compounds at 1 atm pressure

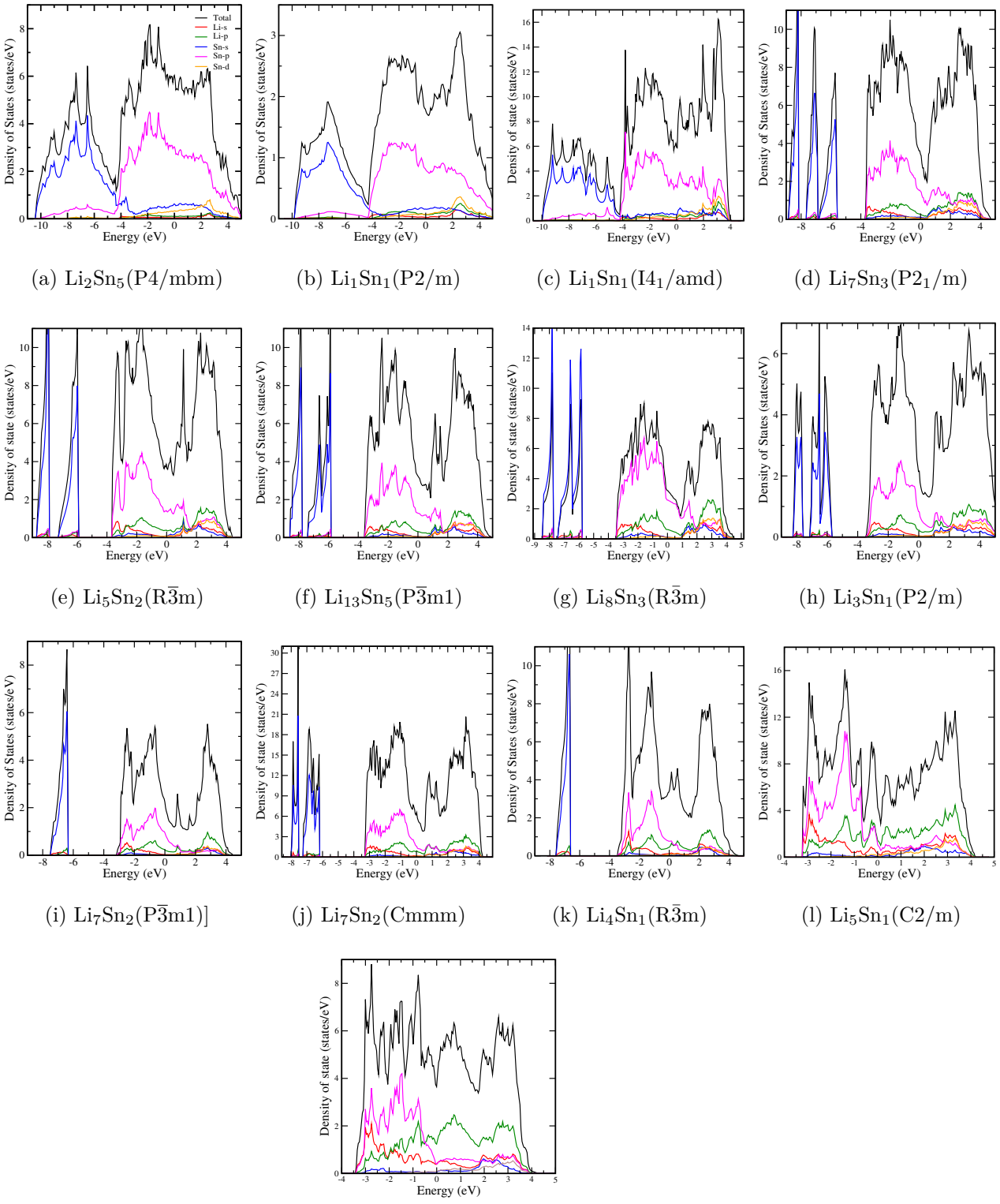

(a) Li_2Sn_5(P4/mbm) (b) Li_1Sn_1(P2/m) (c) Li_1Sn_1($I4_1$/amd) (d) Li_7Sn_3($P2_1$/m)

(e) Li_5Sn_2(R$\bar{3}$m) (f) $Li_{13}Sn_5$(P$\bar{3}$m1) (g) Li_8Sn_3(R$\bar{3}$m) (h) Li_3Sn_1(P2/m)

(i) Li_7Sn_2(P$\bar{3}$m1)] (j) Li_7Sn_2(Cmmm) (k) Li_4Sn_1(R$\bar{3}$m) (l) Li_5Sn_1(C2/m)

(m) Li_7Sn_1(C2/m)

Figure S12: Total and local DOS of: (a) Li_2Sn_5(P4/mbm), (b) Li_1Sn_1(P2/m), (c) Li_1Sn_1($I4_1$/amd), (d) Li_7Sn_3($P2_1$/m), (e) Li_5Sn_2(R$\bar{3}$m), (f) $Li_{13}Sn_5$(P$\bar{3}$m1), (g) Li_8Sn_3(R$\bar{3}$m), (h) Li_3Sn_1(P2/m), (i) Li_7Sn_2(P$\bar{3}$m1), (j) Li_7Sn_2(Cmmm), (k) Li_4Sn_1(R$\bar{3}$m), (l) Li_5Sn_1(C2/m) and (m) Li_7Sn_1(C2/m), compounds at 1 atm pressure.

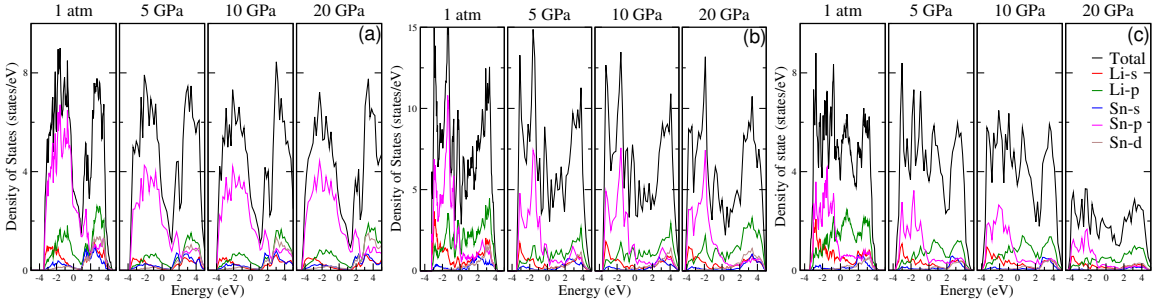

Figure S13: Total and partial density of states (DOS) of: (a) Li_8Sn_3, (b) Li_5Sn_1, and (c) Li_7Sn_1, at 1 atm, 5, 10, and 20 GPa pressure.

Figure S12 in SI depicts the calculated total electronic density of states (DOS) along with the atom resolved partial density of states (PDOS) of all the phases at 1 atm. The crossover of several bands at Fermi level (E_F, set to zero) indicate all Li-Sn compounds to exhibit metallic nature, thus, providing a better electrical conductivity. For most of the Li-Sn phases, the PDOS show a large overlap between Sn-5p and Li-2s and/or Li-2p states at the Fermi level, which illustrates the charge transfer from Li-2s and/or Li-2p to Sn-5p. One can see that the main contribution to total DOS near E_F comes from the Sn-5p state but, as expected this gets weaken with the increase in Li-concentration, which is also in agreement with the work of Zhang et al.[19] on Li-Sn systems at ambient conditions. Moreover, this is also very similar to what is observed recently by Zhang et al.[20] and Yang et al.[21] for Li-Si and Li-Au systems at high pressure, respectively. Finally, in Li-rich phases where $x \geq 4$, Li-2s and Li-2p states dominate and provide major contribution to the total DOS near E_F, as compared to Sn-5p state, owing to the exceptionally high concentration of Li (Figure S12 in SI). In order to determine the effect of pressure on density of states, we present DOS for three of the yet unexplored compounds (Li_8Sn_3, Li_5Sn_1, and Li_7Sn_1) at different pressure values in Figure S13. It is evident from the figure that the nature of DOS is mainly insensitive to the applied pressure. The application of pressure in GPa though decreases the intensity of peaks (density/states) as compared to 1 atm pressure, but other than that no distinct change is noticed for any particular phase within the pressure value of 5–20 GPa.

14. Theoretical XRD pattern of different Li-Sn compounds

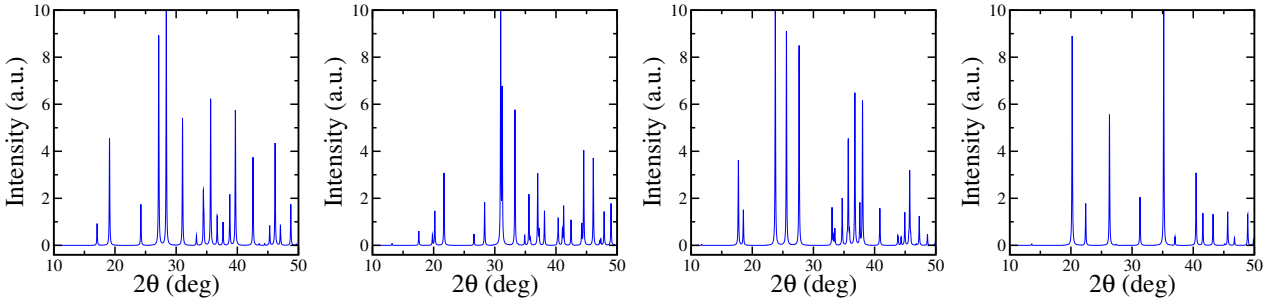

(a) Li_2Sn_5(P4/mbm) (b) Li_2Sn_5(Pbam) (c) Li_1Sn_1(P2/m) (d) Li_1Sn_1($I4_1$/amd)

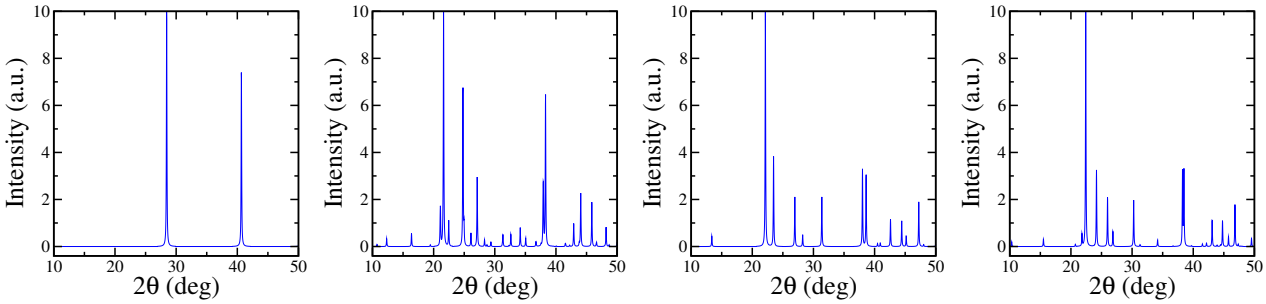

(e) Li_1Sn_1($Pm\bar{3}m$) (f) Li_7Sn_3($P2_1$/m) (g) Li_5Sn_2($R\bar{3}m$) (h) $Li_{13}Sn_5$($P\bar{3}m1$)

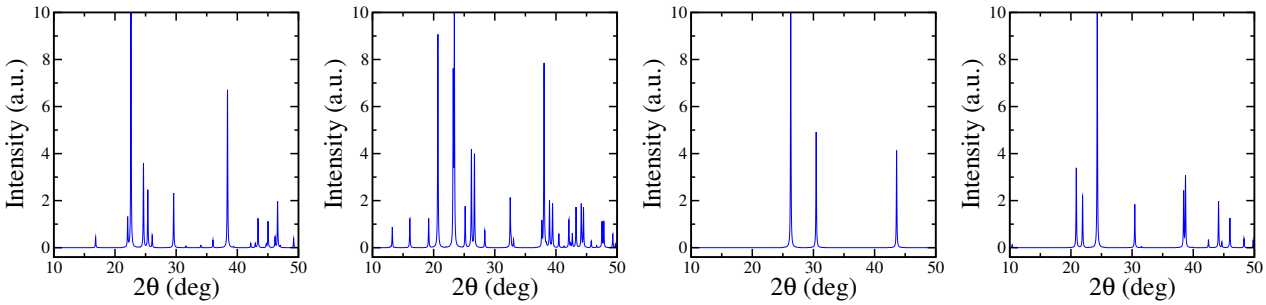

(i) Li_8Sn_3($R\bar{3}m$) (j) Li_3Sn_1(P2/m) (k) Li_3Sn_1($Fm\bar{3}m$) (l) Li_7Sn_2($P\bar{3}m1$)

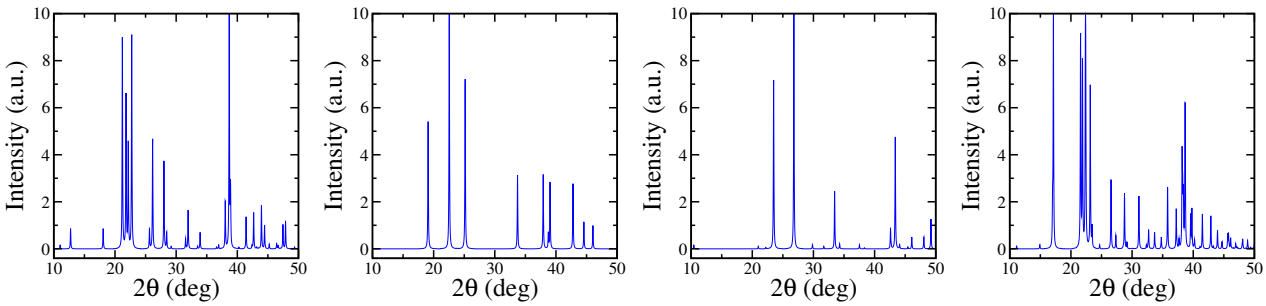

(m) Li_7Sn_2(Cmmm) (n) Li_4Sn_1($R\bar{3}m$) (o) Li_4Sn_1(I4/m) (p) Li_5Sn_1(C2/m)

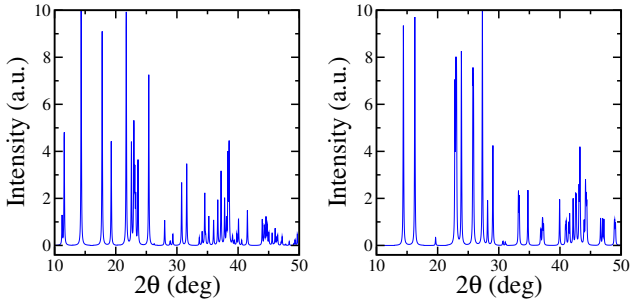

(q) $Li_7Sn_1(C2/m)$ (r) $Li_7Sn_1(P\bar{1})$

Figure S14: Theoretical X-ray diffraction pattern of: (a) $Li_2Sn_5(P4/mbm)$, (b) $Li_2Sn_5(Pbam)$, (c) $Li_1Sn_1(P2/m)$, (d) $Li_1Sn_1(I4_1/amd)$, (e) $Li_1Sn_1(Pm\bar{3}m)$, (f) $Li_7Sn_3(P2_1/m)$, (g) $Li_5Sn_2(R\bar{3}m)$, (h) $Li_{13}Sn_5(P\bar{3}m1)$, (i) $Li_8Sn_3(R\bar{3}m)$, (j) $Li_3Sn_1(P2/m)$, (k) $Li_3Sn_1(Fm\bar{3}m)$, (l) $Li_7Sn_2(P\bar{3}m1)$, (m) $Li_7Sn_2(Cmmm)$, (n) $Li_4Sn_1(R\bar{3}m)$, (o) $Li_4Sn_1(I4/m)$ (p) $Li_5Sn_1(C2/m)$, (q) $Li_7Sn_1(C2/m)$ and $Li_7Sn_1(P\bar{1})$, studied in these work. The wavelength of Cu K_α radiation is used for simulations of XRD pattern *via* Mercury software.[9]

[1] Zhang, W.; Oganov, A. R.; Goncharov, A. F.; Zhu, Q.; Boulfelfel, S. E.; Lyakhov, A. O.; Stavrou, E.; Somayazulu, M.; Prakapenka, V. B.; Konôpková, Z. Unexpected Stable Stoichiometries of Sodium Chlorides. *Science* 2013, *342*, 1502-1505.

[2] Zeng, Z.; Zeng, Q.; Liu, N.; Oganov, A. R.; Zeng, Q.; Cui, Y.; Mao, W. L. A Novel Phase of $Li_{15}Si_4$ Synthesized Under Pressure. *Adv. Energy Mater.* 2015, *5*, 1500214.

[3] Kresse, G.; Furthmuller, J. Efficient Iterative Schemes for *ab initio* Total-Energy Calculations using a Plane-Wave Basis Set. *Phys. Rev. B* 1996, *54*, 11169-11186.

[4] Kresse, G.; Furthmuller, J. Efficiency of *ab-initio* Total Energy Calculations for Metals and Semiconductors using a Plane-Wave Basis Set. *Comput. Mater. Sci.* 1996, *6*, 15-50.

[5] Blöchl, P. E. Projector Augmented-Wave Method. *Phys. Rev. B* 1994, *50*, 17953-17979.

[6] Perdew, J. P.; Burke, K.; Ernzerhof, M. Generalized Gradient Approximation Made Simple. *Phys. Rev. Lett.* 1996, *77*, 3865-3868.

[7] Togo, A.; Oba, F.; Tanaka, I. First-Principles Calculations of the Ferroelastic Transition between Rutile-type and $CaCl_2$-type SiO_2 at High Pressures. *Phys. Rev. B* 2008, *78*, 134106.

[8] Hill, R. The Elastic Behaviour of a Crystalline Aggregate. *Proceedings of the Physical Society. Section A* 1952, 65, 349-354.

[9] Macrae, C. F.; Bruno, I. J.; Chisholm, J. A.; Edgington, P. R.; McCabe, P.; Pidcock, E.; and Rodriguez-Monge, L.; Taylor, R.; van de Streek, J.; Wood, P. A. *Mercury CSD 2.0* - New Features for the Visualization and Investigation of Crystal Structures. *J. Appl. Crystallogr.* 2008, *41*, 466-470

[10] Hansen, D.A.; Chang, L. J. Crystal Structure of Li_2Sn_5 *Acta Cryst.* 1969, *B25*, 2392-2395.

[11] Müller, W.; Schäfer, H. The Crystal Structure of LiSn. *Z. Naturforsch.* 1973, *28b*, 246-248.

[12] Blase, W.; Cordier, G. Crystal Structure of β-Lithium stannide, β-LiSn. *Zeitschrift für Kristallographie* 1990, *193*, 317-318.

[13] Müller, W. Preparation and Crystal Structure of Li_7Sn_3. *Z. Naturforsch.* 1974, *29b*, 304-307.

[14] Frank, U.; Müller, W.; Schäfer, H. The Crystal Structure of Li_5Sn_2. *Z. Naturforsch.* 1975, *30b*, 1-5.

[15] Frank, U.; Müller, W.; Schäfer, H. The Crystal Structure of Li_7Sn_2. *Z. Naturforsch.* 1975, *30b*, 6-9.

[16] Frank, U.; Müller, W. The Preparation and Crystal Structures of $Li_{13}Sn_5$ and Structural Relations between the Phases of the Systems Li-Sn and Li-Pb. *Z.Naturforsch.* 1975, *30b*, 316-322.

[17] Genser, O.; Hafner, J. Structure and Bonding in Crystalline and Molten Li-Sn Alloys: A First-Principles Density-Functional Study. *Phys. Rev. B* 2001, *63*, 144204.

[18] Morris, A. J.; Grey, C. P.; Pickard, C. J. Thermodynamically Stable Lithium Silicides and Germanides from Density Functional Theory Calculations. *Phys. Rev. B* 2014, *90*, 054111.

[19] Zhang, P.; Ma, Z.; Wang, Y.; Zou, Y.; Lei, W.; Pan, Y.; Lu, C. A First Principles Study of the Mechanical Properties of Li-Sn Alloys. *RSC Adv.* 2015, 5, 36022-36029

[20] Zhang, S.; Wang, Y.; Yang, G.; Ma, Y. Silicon Framework-Based Lithium Silicides at High Pressures. *ACS Appl. Mater. Interfaces* 2016, *8*, 16761-16767.

[21] Yang, G.; Wang, Y.; Peng, F.; Bergara, A.; Ma, Y. Gold as a 6p-Element in Dense Lithium Aurides. *J. Am. Chem. Soc.* 2016, *138*, 4046-4052.